Cancer Letters 448 (2019) 132–143

Contents lists available at ScienceDirect

Cancer Letters

journal homepage: www.elsevier.com/locate/canlet

Original Articles

Targeted demethylation of the *SARI* promotor impairs colon tumour growth

Qin Wang[a,1], Lei Dai[a,**,1], Yuan Wang[a], Jie Deng[a], Yi Lin[a], Qingnan Wang[a], Chao Fang[b], Zida Ma[b], Huiling Wang[a], Gang Shi[a], Lin Cheng[a], Yi Liu[a], Shuang Chen[a], Junshu Li[a], Zhexu Dong[a], Xiaolan Su[a], Lie Yang[b], Shuang Zhang[c], Ming Jiang[c], Meijuan Huang[c], Yang Yang[a], Dechao Yu[a], Zongguang Zhou[b], Yuquan Wei[a], Hongxin Deng[a,*]

[a] *State Key Laboratory of Biotherapy and Cancer Center, West China Hospital, Sichuan University and Collaborative Innovation Center for Biotherapy, Chengdu, Sichuan, 610041, PR China*

[b] *Department of Gastrointestinal Surgery, West China Hospital and State Key Laboratory of Biotherapy, Sichuan University, Chengdu, Sichuan, 610041, PR China*

[c] *Cancer Center, West China Hospital, Sichuan University and Collaborative Innovation Center for Biotherapy, Chengdu, Sichuan, 610041, PR China*

ARTICLE INFO

Keywords:
Colon cancer
SARI
Methylation
dCas9
TET1

ABSTRACT

SARI (suppressor of activator protein 1, regulated by IFN) functions as a tumour suppressor and is inactivated in various cancers. However, the mechanism underlying SARI inactivation in cancer remains elusive. In this study, we detected a high level of DNA methylation of the *SARI* promoter and an inverse correlation between *SARI* promoter methylation and expression in malignant tissues from patients with colon cancer. Furthermore, we found that the *SARI* promoter methylation status is a prognostic indicator for patients with colon cancer. A dCas9-multiGCN4/scFv-TET1CD-sgRNA-based *SARI*-targeted demethylation system (dCas9-multiGCN4/scFv-TET1CD-sgSARI) was constructed to precisely and specifically demethylate regions of *SARI*; this system resulted in the substantial activation of SARI expression. Further *in vitro* and *in vivo* data confirmed that dCas9-multiGCN4/scFv-TET1CD-sgSARI exerts anti-tumour effects by regulating tumour proliferation, apoptosis, and angiogenesis. Collectively, specific demethylation of the *SARI* promoter and restoration of endogenous SARI expression by dCas9-multiGCN4/scFv-TET1CD-SARI have therapeutic applications for colon cancer and perhaps for other cancers.

1. Introduction

DNA methylation has an important physiological role in transcriptional regulation, and alterations in methylation result in pathological conditions, such as cancer development and progression [1–3]. Thus, the inhibition of DNA methylation is a promising approach for cancer therapy [3,4]. 5-aza-2′-deoxycytidine (DAC), a broad-spectrum agent for DNA demethylation, showed anti-leukaemic effects in several clinical trials and has been approved by the FDA for the treatment of myelodysplastic syndromes [5,6]. However, the global demethylation process has undesirable effects, and this low specificity limits the use of DAC or 5-azacytidine (AZA) in clinical settings [7,8].

To dissect the functional significance of DNA methylation events in the human genome, zinc-finger nucleases (ZFNs) [9], transcription activator-like effector (TALE) [10], and CRISPR–Cas9 [11–13] have been used for targeted epigenome editing by fusion with epigenome-modifying enzymes. Recently, many enzymes, including TET (ten eleven translocation), have been found to catalyse active DNA demethylation via distinct mechanisms [14]. Among these, TET1 is a dioxygenase that catalyses the hydroxylation of 5-methylcytosine to 5-hydroxymethylcytosine and the subsequent generation of 5-formylcytosine and 5-carboxylcytosine with the TET catalytic domain (TET-CD) as the smallest functional module [15]. A catalytically inactive Cas9 (dCas9)-based system fused to the catalytic domain of TET1 (TET1CD) that hydroxylates specific loci has been designed to activate site-specific demethylation [12,16,17].

Suppressor of activator protein 1, regulated by IFN (*SARI*; also known as *BATF2*) is located on human chromosome 11q (mouse

* Corresponding author. State Key Laboratory of Biotherapy and Cancer Center, West China Hospital, Sichuan University and Collaborative Innovation Center for Biotherapy, Ke-yuan Road 4, No. 1, Gao-peng Street, Chengdu, Sichuan, 610041, PR China.

** Corresponding author. State Key Laboratory of Biotherapy and Cancer Center, West China Hospital, Sichuan University and Collaborative Innovation Center for Biotherapy, Ke-yuan Road 4, No. 1, Gao-peng Street, Chengdu, Sichuan, 610041, PR China.

E-mail addresses: dailei2016@scu.edu.cn (L. Dai), denghongx@scu.edu.cn (H. Deng).

[1] These authors contributed equally to this work.

https://doi.org/10.1016/j.canlet.2019.01.040
Received 25 October 2018; Received in revised form 23 January 2019; Accepted 29 January 2019

chromosome 19) and belongs to the *BATF* family, which includes *BATF1* and *BATF3*. SARI was initially identified as a regulator involved in immune responses [18], similar to BATF1 and BATF3 [19]. SARI induces the production of inflammatory and host-protective proteins, e.g. TNF, Ccl5, and Nos2, by directly targeting Irf1 during *Mycobacterium tuberculosis* infection [20]. SARI additionally controls Th17-mediated immunopathology by suppressing IL-23 production during *Trypanosoma cruzi* infection in innate immune cells [21]. In cancers, the ectopic expression of SARI significantly inhibits tumour cell proliferation and the epithelial–mesenchymal transition and induces apoptosis [22–28]. SARI also has an anti-tumour effect via the up-regulation of IL-12 p40 in TAMs, which eventually induces $CD8^+$ T-cell activation and accumulation within the tumour [29]. We have also shown that SARI inhibits angiogenesis by directly targeting the ceruloplasmin and inhibiting the HIF-1α/VEGF axis in colon cancer [30]. Furthermore, SARI is downregulated in malignant tissues and its expression is inversely correlated with clinical outcomes in patients in various cancers, including colon cancer [27,30], B lymphoma [26], and lung cancer [28]. However, the mechanism underlying SARI downregulation in malignant tissues remains unclear.

In the present study, we found that SARI downregulation in colon cancer is DNA methylation-dependent and *SARI* promoter methylation is inversely correlated with the prognosis of patients with colon cancer. We employed a dCas9-multiGCN4/scFv-TET1CD-sgRNA-based targeted demethylation system to restore SARI expression and demonstrated its effectiveness and specificity. dCas9-multiGCN4/scFv-TET1CD-sgSARI had anti-tumour roles *in vitro* and *in vivo* by regulating the expression of downstream targets in colon cancer.

2. Methods

2.1. Cell lines and antibodies

All colon cancer cell lines (SW480, HCT116, HT29, RKO and HCT15) were purchased from American Type Culture Collection (ATCC, Manassas, VA, USA) and cultured in DMEM supplemented with 10% fetal bovine serum (FBS) and antibiotics. Cell line authentication was assessed using a short tandem repeat DNA profiling method in our laboratory, and the latest verification was done in July 2017. The mycoplasma detecting kit (catalogue no. MD001), purchased from Shanghai Yise Medical Technology was performed to test whether there are mycoplasma contamination in all cells. HUVECs were maintained as described previously and cultured in EndoGRO-VEGF medium (Millipore, MA, USA) [30].

Antibodies used in this study were as follows: SARI (ab157466, Abcam, London, UK), CD31 (ab28364-100, Abcam, London, UK), HIF-1α (H6536, Sigma, MO, USA), VEGF (ab46154, Abcam), MMP-2(4022, CST, MA, USA), Phospho-*c*-Jun (3270, CST, MA, USA), Met(8198, CST, MA, USA), Phospho-Met(3077, CST, MA, USA), Cleaved Caspase-3(9664, CST, MA, USA), Cyclin D1(2978, CST, MA, USA), MMP-7(71031, CST, MA, USA), c-Jun(9165, CST, MA, USA), GAPDH (sc365062, Santa Cruz Biotechnology).

2.2. Animals

Female BALB/c nude mice were purchased from the Model Animal Research Center of Nanjing University (Nanjing, China) and allowed to acclimate for 1 week before use. All mouse care and experiments were carried out in accordance with institutional guidelines concerning animal use and care of Sichuan University. Control and sgSARI cells (HCT116 and RKO cells) (5×10^6 cells) were injected into the flank of female BALB/c nude mice to establish a subcutaneous cancer model. Tumour size was determined by collecting length and width measurements, and calculating the tumour volume (mm^3) as (tumour length × (tumour width)^2) × 0.52. When mice were killed, tumours from each animal were collected, weighed and used for histopathological studies.

2.3. Construction of targeted demethylation vector

The all in one vector (Addgene plasmid 82559) which contains Cas9 peptide array (linker length: 22aa), antibody-sfGFP-TET1CD, and gRNA expression system [12] was used in the present study. Cloning was performed by linearization of the Addgene plasmid 82559 *Afl*II site and Gibson assembly-mediated incorporation of the gRNA insert fragment. Mix the plasmid 82559 digested with *Afl*II (50 ng) with 1 μl insert oligonucleotide mixture, 6 μl 2 × Gibson Assembly Master Mix, and H_2O to adjust the volume to 10 μl. Incubate at 50 °C for 15 min. Perform bacterial transformation using 5 μl reaction mixture described above into competent *Escherichia coli*, and spread them over solid medium containing kanamycin to select for successfully transformed clones. Culture the colony and purify the plasmid. The target sequences are described in Supplementary Sequences.

2.4. Cell transfection

In demethylation experiments, cells were seeded in 12-well format (Corning) and the plasmids were transfected into cells using X-tremeGENE HP DNA Transfection Reagent (Roche), respectively, according to the manufacturer's protocols. Cells were harvested 4 days after transfection. To establish the cell lines that stably expressed the demethylation system, cells were subjected to sustained G418 treatment (1000 μg ml^{-1}, medium change per 3 days). Colonies were picked and harvested for RNA and genomic DNA extraction to examine the expression and DNA demethylation of the targeted genes.

2.5. RT–PCR and real-time PCR

Total RNA was extracted from cells using TRIzol reagent (Invitrogen, Carlsbad, CA, USA). RNA samples (1 mg) were subjected to RT–PCR using the TaKaRa One-step RT-PCR kit (Takara, Shiga, Japan). All PCR products were separated by electrophoresis in 1% agarose gels and were visualized using GoldView. For real-time PCR, resulting complementary DNA was analysed in triplicate using SYBR Green (Takara) with the following PCR conditions:95 °C for 150 s; 40 cycles of 95 °C for 10 s, 58 °C for 30 s; 95 °C for 10 s, 65 °C for 60 s, 97 °C for 1 s. All transfections were done in triplicate and for each biological replicate at least three technical replicates of the qPCR assay were done. Statistical significance was determined by comparing experimental samples against the off-target con-trol using a one-sided *t*-test after confirming that data sets exhibited a normal distribution as determined by a Shapiro-Wilk test for normality ($P < 0.05$).

2.6. Western blotting

After plasmid transfection, cells were collected and lysed on ice for 30 min with the RIPA lysis buffer (Beyotime, Nanjing, China) containing 1% protease inhibitor cocktail (Merck Millipore). The lysis was centrifuged for 15 min by 12,000 g at 4 °C, and the supernatants were collected. The Bradford protein assay kit (Thermo Scientific, MA, USA) was employed to determine the protein concentrations. An amount of 20 μg protein with equal amount was loaded and separated by SDS–PAGE gel electrophoresis, followed by the transfer of proteins onto the polyvinylidenedi fluoride membranes (Merck Millipore). After blocking with TBS/T buffer containing 5% milk, the membranes were incubated with the primary antibodies against SARI (1:400, Abcam) and GAPDH (1:50,000, CST) in 5% milk TBS/T buffer overnight at 4 °C. Following incubation with horseradish peroxidase-conjugated secondary antibodies (Zsbio, Beijing, China) at room temperature for 1 h, the bands were detected using a chemiluminescent substrate ECL kit (Merck Millipore).

2.7. DNA methylation analysis

Genomic DNA was extracted from cells and tissues with Tissues & Cell Genomic DNA Purification Kit (DP021, GeneMark) and treated with the CpGenome Turbo Bisulfite Modification Kit (Merck KGaA) according to the manufacturer's instruction. The modified DNA was amplified with the PCR primers described in Supplementary Table S4. For methylation analysis of the surrounding area, bisulfite sequencing analysis was performed. Briefly, amplified fragments were ligated into the TOPO vector (TsingKe) and at least 5 clones were sequenced. Sequences were analysed by the methylation analysis tool QUantification tool for Methylation Analysis (QUMA). We used pyrosequencing analysis(Oebiotech) both in order to study this simple and efficient method for a potential clinical use, as well as to quantitatively assess the methylation level of tissue samples and correlate them with overall survival of our patients. After bisulfite conversion of the target sequences, two CpG sites were analysed by pyrosequencing. In brief, double stranded PCR products were denatured with NaOH and washed before a sequencing primer was annealed. The pyrosequencing reaction started at the 3′-end of the sequencing primer. Nucleotides (A, T, C, and G) were dispensed into each sample well, one at a time. Whenever a base complementary to the base in the PCR product was added, it was incorporated into the growing DNA strand, resulting in an enzymatic cascade and production of light. The light intensity was measured at each dispensation and presented graphically in a program. Methylation data are presented as percentage of average methylation in all observed CpG sites.

2.8. Cell proliferation assays

Cells were seeded at a density of 2000 cells per well in 96-well plates and incubated. 10 μl Cell Counting Kit-8 (Dojindo) was added to the wells and incubated for 2 h. The absorbance was measured at 450 nm to calculate the numbers of viable cells in each well. Each measurement was performed in triplicate and the experiments were repeated twice.

2.9. Colony formation assays

For colony formation assays, cells were seeded in six-well plates at a density of 500 cells per well and cultured at 37 °C for two weeks. At the end of the incubation, the cells were fixed with 4% paraformaldehyde and stained with 0.1% (w/v) Crystal Violet. Each measurement was performed in triplicate and the experiments were each conducted at least three times.

2.10. HUVEC tube formation assays

A total of 2×10^5 control and sgSARI cells were plated in the well of a six-well plate with 2 ml of DMEM medium containing 10% FBS. And 48 h later, the conditioned medium was collected and used for *in vitro* tube formation. For the tube formation assay, the wells of a 96-well plate were coated with 50 ml ice-cold BD Matrigel (BD Biosciences). HUVECs (20,000) in 100 ml of conditioned medium were added into the well that plated with Matrigel. HUVECs were incubated for 4–6 h at 37 °C and then visualized by light microscopy. The amount of branch points (≥3 cells per branch) were counted and analysed in five random fields per replicate.

2.11. Migration and invasion assays

Cell migration assay: 5×10^4 cells were suspended in 200 μl serum-free DMEM medium and seeded into the upper chamber of each insert. Then, 500 μl of DMEM containing 10% FBS was added to a 24-well plate. After incubation at 37 °C, the cells that migrated were fixed and stained for 30 min in a 0.1% Crystal Violet solution in PBS.

Cell invasion assay: chambers were uniformly covered with 60 μL Matrigel diluted with DMEM to a certain percentage and incubated at 37 °C for 2–4 h. Then, 5×10^4 cells were suspended in 200 μL DMEM and seeded in the upper chambers, and 500 μl DMEM containing 10% FBS was added to the lower chamber. After incubation at 37 °C, the cells were fixed and stained.

2.12. Immunofluorescence analysis

4% paraformaldehyde was employed to fix the sections at room temperature for 10 min. Then, the sections were blocked with goat serum and incubated with primary antibodies against CD31 (1:400, Abcam, London, UK) for 1.5 h at 37 °C, followed directly by Texas Red-conjugated secondary antibodies (1:500, CST, MA, USA) for 1.5 h at 37 °C. Nuclei were counterstained with DAPI (Roche, Basel, Switzerland). All specimens were evaluated using an Olympus BX600 microscope and SPOT Flex camera.

2.13. Immunohistochemical (IHC) staining

Paraffin sections were used for immunohistochemical analysis. Tumour tissue sections were deparaffinized, rehydrated, and antigen retrieved. Then, the sections were incubated with primary antibodies against SARI (1:100, Abcam), Ki67 (1:300, Abcam) and Caspase 3 (1:100, CST) in a moisture chamber overnight at 4 °C. The next day, cells were incubated with secondary antibody for 2 h. We visualized staining using DAB. Positive cells were indicated by the presence of brown staining in both the nucleus and cytoplasm.

2.14. Apoptosis detection

For Annexin V-FITC/PI Staining(KeyGEN), cells were seeded in a 6-well plate. After 48 h, the cellswere harvested by trypsinization, washed with PBS twice and re-suspended in 500 μl binding buffer. Annexin V-FITC (5 μl) and propidium iodide (5 μl) were added to cell suspension for 5min in the dark at room temperature. The cells were analysed by flow cytometry (ACEA NovoCyte).

2.15. Transcription array

Total RNA was prepared with TRIzol. Total RNA was extracted using the mirVana miRNA Isolation Kit (Ambion) following the manufacturer's protocol. RNA integrity was evaluated using the Agilent 2100 Bioanalyzer (Agilent Technologies, Santa Clara, CA, USA). The samples with RNA Integrity Number (RIN) ≥ 7 were subjected to the subsequent analysis. The libraries were constructed using TruSeq Stranded mRNA LTSample Prep Kit (Illumina, San Diego, CA, USA) according to the manufacturer's instructions. Then these libraries were sequenced on the Illumina sequencing platform (Illumina HiSeq X Ten) and 150bp paired-end reads were generated. All of the procedures were performed by Chengdu Basebiotech Co., Ltd (Chengdu, China). All of the original data of the transcription array was uploaded into NCBI (SRA accession number: SRP158316).

2.16. Statistical analysis

All experiments were repeated three to five times, and the data were expressed as the mean ± s.d. Statistical analysis was performed by the Student's t-tests for comparing two groups and by analysis of variance for multiple group comparisons; $P < 0.05$ was considered statistically significant. Kaplan–Meier curves and the log-rank test were used to compare survival times among the groups. The Pearson correlation analysis was performed to determine the correlation among the groups. All calculations were performed using SPSS v19.0 (SPSS Inc., Chicago, IL, USA).

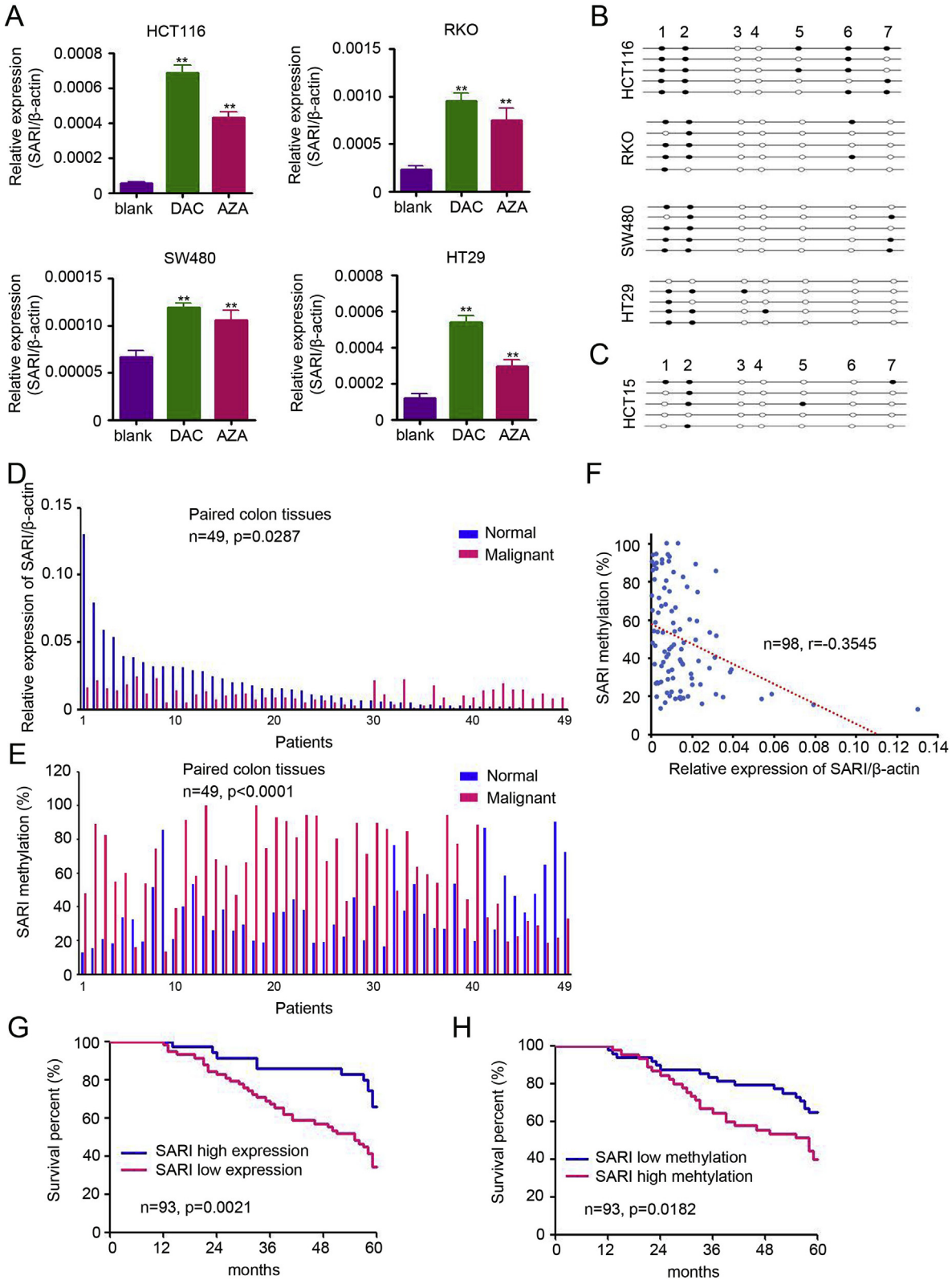

Fig. 1. SARI downregulation is dependent on DNA methylation in colon cancer. (A) *SARI* mRNA expression in colon cancer cells after DAC and AZA treatment. Data are shown after normalization to β-actin (n = 3, **, p < 0.01, compared with the blank group). (B − C) Genomic DNAs extracted from colon cancer cells were treated with bisulfite and then subjected to methylation-specific PCR. Using the PCR productions, the 7 CpG sites located between nucleotides −221 and 193 of *SARI* were sequenced. The horizontal dots represent CpG islands, and the vertical dots represent the 5 individual clones sequenced. (D) *SARI* mRNA expression in paired colon cancer tissues (n = 49). (E) *SARI* promoter methylation status in paired colon cancer tissues (n = 49). SARI methylation was determined by pyrosequencing. (F) Correlation between *SARI* mRNA expression and promoter methylation in colon tissues (Pearson correlation, p < 0.0001, $r = -0.3545$). (G) Kaplan–Meier curve showing the overall survival of patients (in percentage) with colon cancer, stratified by SARI expression (high- and low-expression tumours; n = 93; p = 0.0021; long-rank test). (H) Kaplan–Meier curve showing the overall survival of patients (as percentages) with colon cancer, stratified by SARI methylation (high- and low-methylation tumours; n = 93; p = 0.0182; long-rank test).

3. Results

3.1. DNA methylation mediates SARI downregulation in colon cancer

In a previous study, we found that SARI is downregulated in most colon malignant tissues and colon cancer cells [30]. To determine the potential role of DNA methylation in SARI downregulation, the demethylation agents DAC and AZA were used to treat colon cancer cells (HCT116, RKO, SW480, and HT29). We observed higher *SARI* mRNA expression levels after DAC and AZA treatment than in untreated control cells (Fig. 1A). Genomic DNA extracted from colon cancer cells was treated with bisulfite and then subjected to methylation-specific PCR (MSP) (Supplementary Table 1). After sequencing the MSP products, three out of seven CpG sites were methylated in colon cancer cells with low or no SARI expression; these sites were located between nucleotides −221 and 193 of *SARI* (Fig. 1B). The few precise number of methylated CpG sites were found in HCT15 colon cancer cells (Fig. 1C), which exhibit high SARI expression. Quantitative real-time PCR results demonstrated that *SARI* was downregulated in 67.35% of human colon tumour tissues, compared with levels in adjacent normal tissues (Fig. 1D, Normal: 0.01857 ± 0.00337 vs. Malignant: 0.01083 ± 0.00087, $p = 0.0287$). A higher methylation percentage was found in malignant tissues (Fig. 1E; Normal: 37.07 ± 1.09% vs. Malignant: 52.85 ± 2.63%, $p < 0.0001$). Indeed, the mean percentage of CpG methylation (Fig. 1F) in SARI was inversely correlated with the expression level (Pearson's $r = -0.3545$, $p < 0.0001$, Fig. 1F), suggesting that DNA methylation represses *SARI* transcription in human colon tumours. These results suggested that SARI downregulation in human colon tumour tissues is DNA methylation-dependent.

3.2. SARI methylation is a prognostic indicator for patients with colon cancer

We previously demonstrated that SARI protein expression is inversely correlated with poor prognosis in patients with colon cancer [30]. The SARI mRNA expression and methylation was determined in the present study and divided as “low” and “high” according to the average value. The present results suggested that *SARI* mRNA expression is a positive prognostic indicator for patients with colon cancer ($n = 93$, $p = 0.0021$, Fig. 1G). Furthermore, SARI methylation has a predictive role in patients with colon cancer ($n = 93$, $p = 0.0182$, Fig. 1H). The detailed correlations between clinicopathological characteristics and the expression of SARI are listed in Supplementary Table 2.

3.3. Selective demethylation of SARI in colon cancer cells upon transfection with dCas9-multiGCN4/scFv-TET1CD-sgRNA

To reverse SARI expression by demethylation, seven sgRNAs (Supplementary Table 3) designed to target the *SARI* region from −418 bp to 152 bp were used to construct a dCas9-multiGCN4/scFv-TET1CD-sgRNA-based specific demethylation system [12] (Fig. 2A). After the transfection of HCT116 cells with dCas9-multiGCN4/scFv-TET1CD-sgSARI, the greatest increases in *SARI* transcription were detected for sgSARI-1, -4, and -5 (Fig. 2B). Among these, dCas9-multiGCN4/scFv-TET1CD-sgSARI-1 and dCas9-multiGCN4/scFv-TET1CD-sgSARI-5, which caused the greatest increases, were selected for further analyses. Quantitative real-time PCR and western blotting results confirmed the efficient upregulation of SARI at the mRNA and protein levels in several colon cancer cells (HCT116, RKO, SW480, HT-29; Fig. 2C&D). MSP product-based sequencing also demonstrated reductions in methylated CpG sites in dCas9-multiGCN4/scFv-TET1CD-sgSARI-1- and dCas9-multiGCN4/scFv-TET1CD-sgSARI-5-transfected colon cancer cells (Fig. 2E).

3.4. Evaluation of the off-target effects of the dCas9-based demethylation system

Off-target effects are a major concern for the practical application of any Cas9-based technique. Thus, the top 10 potential off-target loci according to a COSMID web tool (https://crispr.bme.gatech.deu/) [31] were selected to examine whether their mRNA transcription levels were altered as a result of interference or random demethylation by dCas9-multiGCN4/scFv-TET1CD-sgSARI-1 (Fig. 3A) and dCas9-multiGCN4/scFv-TET1CD-sgSARI-5 (Fig. 3C). As shown in Fig. 3B&D, no significant differences in the mRNA expression levels of these potential off-target genes were detected between the dCas9-multiGCN4/scFv-TET1CD-sgSARI-1 group and dCas9-multiGCN4/scFv-TET1CD-sgRNA (Fig. 3B) or between dCas9-multiGCN4/scFv-TET1CD-sgSARI-5 and dCas9-multiGCN4/scFv-TET1CD-sgRNA (Fig. 3D). Collectively, these results confirmed the specificity of dCas9-multiGCN4/scFv-TET1CD-sgSARI on SARI demethylation.

3.5. Targeted demethylation of SARI impairs colon tumour progression

To determine the potential anti-tumour effect of the targeted demethylation of SARI in colon cancer, dCas9-multiGCN4/scFv-TET1CD-sgSARI-transfected colon cancer cells were used for various *in vitro* experiments. Our results demonstrated the low proliferation activity of HCT116 and RKO cells transfected with dCas9-multiGCN4/scFv-TET1CD-sgSARI-1 or dCas9-multiGCN4/scFv-TET1CD-sgSARI-5 (Fig. 4A), accompanied by an increase in apoptotic cells (Fig. 4B). As shown in Fig. 4C, fewer colonies were found in colon cancer cells with SARI demethylation. A Matrigel-based HUVEC tube formation assay indicated that the targeted demethylation of SARI efficiently inhibits angiogenesis *in vitro* (Fig. 4D). Furthermore, fewer migrated and invaded HCT116 and RKO cells were observed in the dCas9-multiGCN4/scFv-TET1CD-sgSARI-transfected groups than in control groups (Fig. 4E &F). These results demonstrated the anti-tumour effect of the targeted demethylation of SARI in colon cancer.

3.6. Targeted demethylation of SARI inhibits colon tumour growth in vivo

Next, to determine whether the targeted demethylation of SARI influences tumour growth *in vivo*, 5×10^6 HCT116 and RKO cancer cells were injected into the flank of female wild-type (WT) BALB/c nude mice to establish a subcutaneous tumour model. Our results indicated that the targeted demethylation of SARI significantly reduced the tumour volume and weight of HCT116 cells (Fig. 5A&B, tumour volume: sgRNA: 1793.2 ± 120.0 mm^3 versus sgSARI-1: 911.3 ± 61.1 mm^3 and sgSARI-5: 1213.5 ± 80.2 mm^3; tumour weight: sgRNA: 1.045 ± 0.077 g versus sgSARI-1: 0.571 ± 0.038 g and shSARI-5: 0.790 ± 0.060 g). Targeted demethylation of SARI also dramatically inhibited the tumour volume and weight of RKO cells (Fig. 5C&E, tumour volume: sgRNA: 1037.2 ± 117.2 mm^3 versus sgSARI-1: 498.2 ± 64.3 mm^3 and sgSARI-5: 682.6 ± 81.9 mm^3; tumour weight: sgRNA: 0.553 ± 0.049 g versus sgSARI-1: 0.290 ± 0.048 g and shSARI-5: 0.373 ± 0.061 g). SARI staining confirmed that SARI is expressed in dCas9-multiGCN4/scFv-TET1CD-sgSARI-1- or dCas9-multiGCN4/scFv-TET1CD-sgSARI-5-transfected HCT116 cells (Fig. 5E). Additionally, fewer proliferative and more apoptotic cells were observed in HCT116 tumours after the targeted demethylation of SARI (Fig. 5F&G). CD31 staining also suggested that the targeted demethylation of SARI significantly inhibits HCT116 tumour angiogenesis (Fig. 5H). Collectively, these *in vivo* data suggest that the targeted demethylation of SARI is a potential anti-tumour strategy.

3.7. Targeted demethylation of SARI regulates downstream target expression

A transcription array was used to evaluate the deregulation of genes

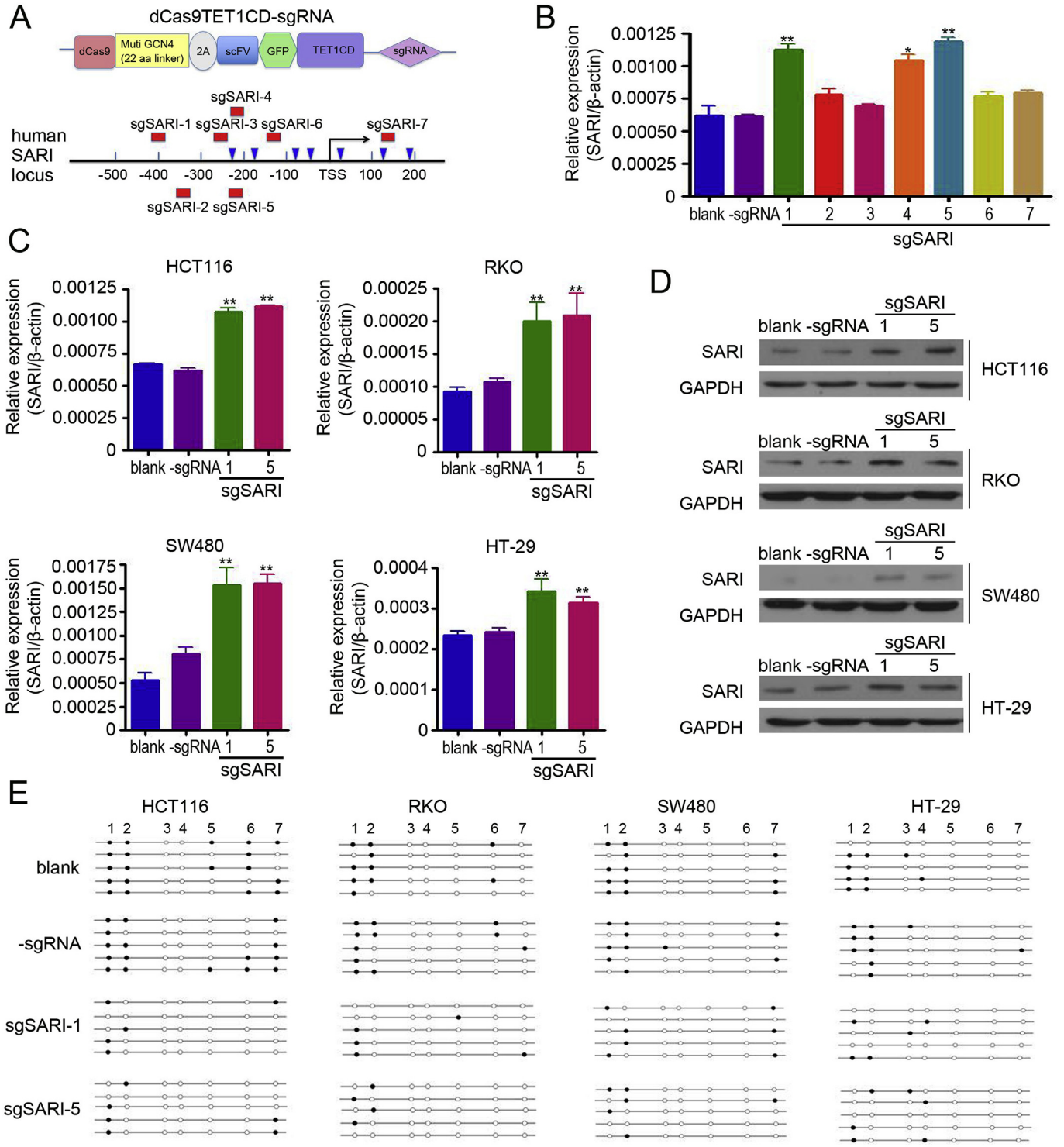

Fig. 2. Demethylation of SARI by dCas9 and sgRNAs. (A) Schematic description of targeted demethylation via dCas9-multiGCN4/scFv-TET1CD-sgRNA. The sgRNAs recognizing respective target sites are shown in red, and CpG sites are indicated with blue arrowheads. (B) *SARI* mRNA expression was determined by quantitative real-time PCR after dCas9-multiGCN4/scFv-TET1CD-sgRNA and dCas9-multiGCN4/scFv-TET1CD-sgSARI (1–7) transfection for 2 days (dCas9-multiGCN4/scFv-TET1CD-sgRNA, cells transfected with dCas9-multiGCN4/scFv-TET1CD but not any sgRNAs targeting SARI sites). (C&D) *SARI* mRNA (C) and protein (D) expression levels were determined by quantitative real-time PCR and western blotting after transfection for 2 days. (E) Genomic DNA extracted from colon cancer cells was treated with bisulfite and then subjected to methylation-specific PCR. The MSP products were sequenced to evaluate the 7 CpG sites located between nucleotides −418bp and 152bp of the *SARI* promoter. The horizontal dots represent CpG islands, and the vertical dots represent the 5 individual clones sequenced.

after the targeted demethylation of SARI in HCT116 cells. We identified 304 downstream genes that were upregulated and 167 downstream genes that were downregulated by dCas9-multiGCN4/scFv-TET1CD-sgSARI (Fig. 6A). A KEGG analysis indicated that the apoptosis and cell cycle pathways, PI3K-Akt signalling pathway, MAPK signalling pathway, VEGF signalling pathway, and ubiquitin-mediated proteolysis were involved in SARI demethylation (Fig. 6B). Western blotting results suggested that the targeted demethylation of SARI inhibited p-*c*-Jun

A

Target Sequence	Chromosome	Strand	Gene	Mismatches	Score
TTCGTGGTGGTGGTATTATCTGG	9	-	TTLL11	3	1.14
TAGGGGGTGATTGTATTATTAAG	15	+	FMN1	3	1.4
TTTGGGTTGGTTTATTATCTGG	19	+	ZNF461	2	1.99
TTGGGGATGATTGTATTTCTGG	10	-	MYO3A	2	5.24
TTGGGGGTATTGTATTCTCAGG	8	+	CSMD1	2	5.36
TTGGGGGTGGTTATTTTATCCAG	14	+	SIPA1L1	2	6
TTGGGGGTGGTTTTACCTATCAGG	3	-	ERC2	2	6.4
TTGGTGGTGGTTGTGTTTCTGG	6	+	UTRN	2	6.6
TTGGGGGTGGATGGATTACGGG	20	+	ZNF831	2	7.51
TTGGGGGTGGTTTATGAACAGG	8	+	MROH1	2	9.61

B

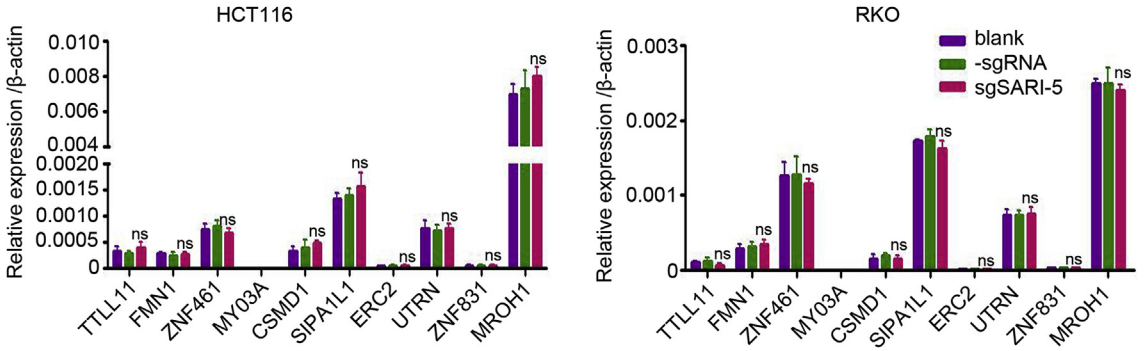

C

Target Sequence	Chromosome	Strand	Gene	Mismatches	Score
ACAAGTGCATGGTCCCCACTGG	1	+	SRGAP2C	2	1.59
ATATGAGCTGGGTCCCCACGGG	7	-	KDELR2	2	1.69
CCATTAGCATCTGGTCCCCACAGG	16	+	ACSM2A	2	1.81
GTGAGGACAGATGCACATGTGGG	8	-	DLGAP2	3	2.42
CTGAGGACCGATGCTGATGTTGG	10	+	PARD3	3	2.59
GTGGGGACCTGTGCCATGTGGG	7	-	PRKAR1B	2	3.61
GTGGGGACCATGCCAATGTGGG	7	+	ZAN	2	5.21
GTGGGAACCGATGCTCCAGGTGGG	11	-	MUC2	2	7.21
GTGAGGACCGATGCTCAGTGAG	11	+	OPCML	2	24.68
GTGGGGACCGTGCTCATGTTCC	9	+	SUSD3	2	41.21

D

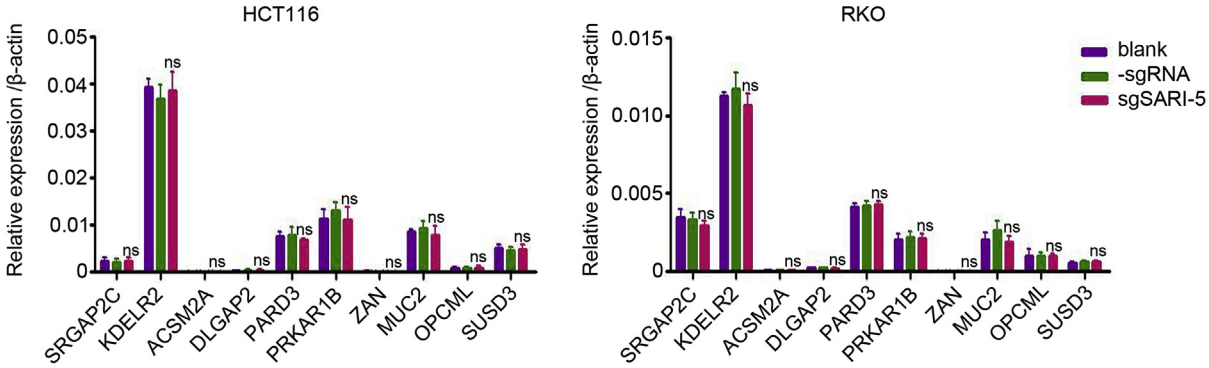

Fig. 3. Assessment of the off-target effects of the dCas9-based demethylation system. (A) The top 10 potential off-target sites predicted for sgSARI-1 were selected using a scoring system described previously [31]. (B) Quantitative real-time PCR analysis of off-target mRNA expression levels in HCT116 and RKO cells transfected with dCas9-TET-sgSARI-1, compared with those for the blank or sgRNA controls Data are shown after normalization to β-actin (n = 3). (C) The top 10 potential off-target sites predicted for sgSARI-5 were selected using a scoring system described previously [31]. (D) Quantitative real-time PCR analysis of off-target mRNA expression levels in HCT116 and RKO cells transfected with dCas9-TET-sgSARI-5, compared with those of the blank or sgRNA controls. Data are shown after normalization to β-actin (n = 3). The primer sequences are listed in Supplementary Table 5.

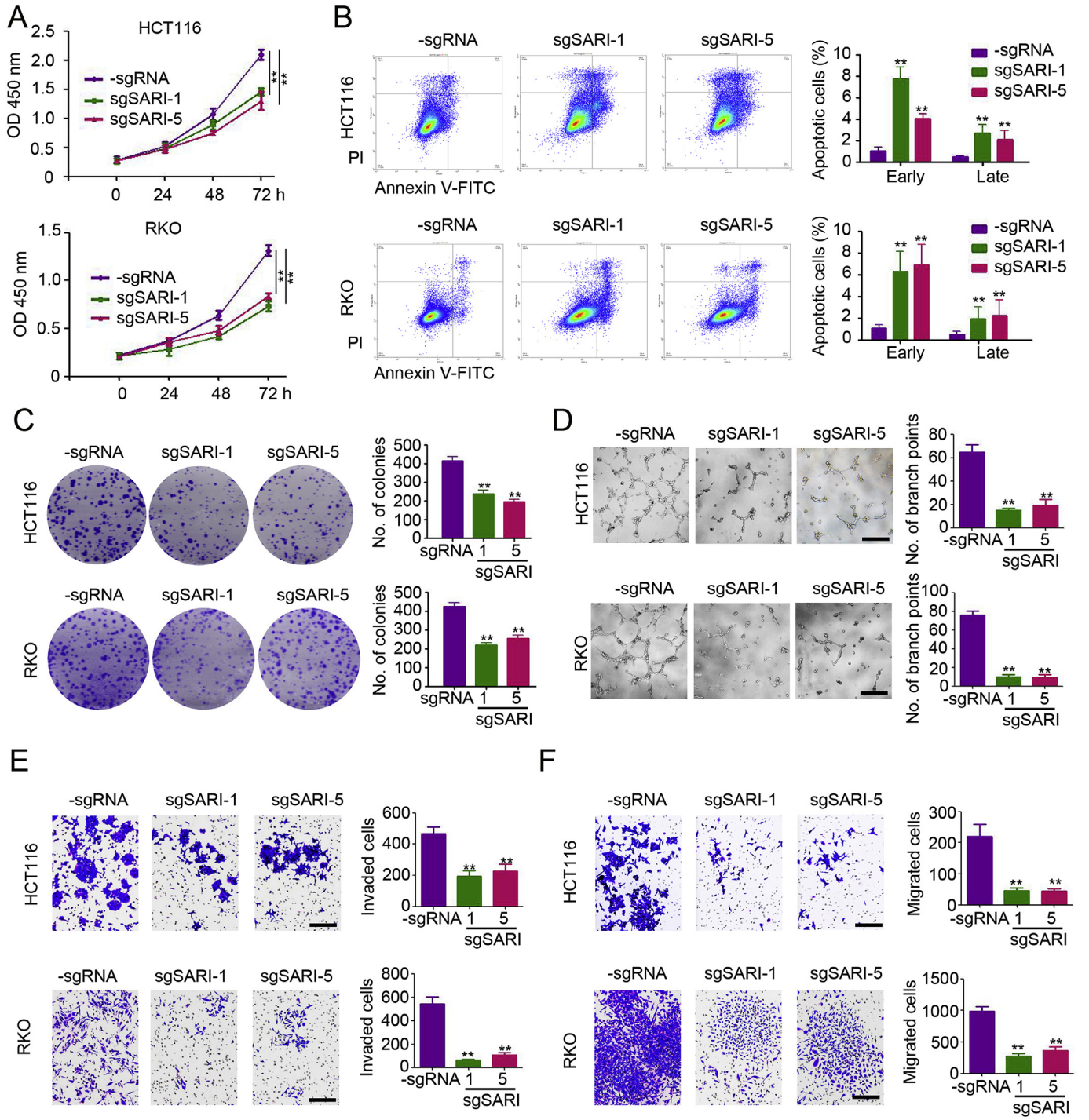

Fig. 4. Antitumour effect of the targeted demethylation of SARI *in vitro*. (A) A Cell Counting Kit-8 (CCK8) assay was performed to determine the growth of HCT116 and RKO cells transfected with dCas9-multiGCN4/scFv-TET1CD-sgRNA, dCas9-multiGCN4/scFv-TET1CD-sgSARI-1, and dCas9-multiGCN4/scFv-TET1CD-sgSARI-5 (n = 5). (B) Flow cytometry was performed to detect apoptotic cells of HCT116 and RKO cells after transfection (n = 5). The percentages of early apoptotic cells (PI^- Annexin V^+) and late apoptotic cells (PI^+ Annexin V^+) were analysed (n = 3). (C) Colony formation assay was performed using HCT116 and RKO cells after transfection. The numbers of colonies per well were counted and analysed (n = 3). (D) The supernatants of HCT116 and RKO cells after transfection were collected for a Matrigel-based HUVEC tube formation assay. The number of branch points per frame were counted and analysed (n = 5). (E) HCT116 and RKO cells after transfection were collected for a Transwell-based migration assay. The migrated cells per frame were counted and analysed (n = 5). (F) HCT116 and RKO cells after transfection were collected for a Matrigel-based invasion assay. The invaded cells per frame were counted and analysed (n = 5).

and CCND1 expression and promoted caspase 3 expression in colon cancer cells (Fig. 6C). Furthermore, reduced levels of MMP-2 and MMP-7 expression were also found in dCas9-multiGCN4/scFv-TET1CD-sgSARI-transfected colon cancer cells (Fig. 6D). Consistent with the inhibitory role of SARI in colon cancer, we found that the targeted demethylation of SARI reduced HIF-1α and VEGF expression in colon cancer cells (Fig. 6E&F).

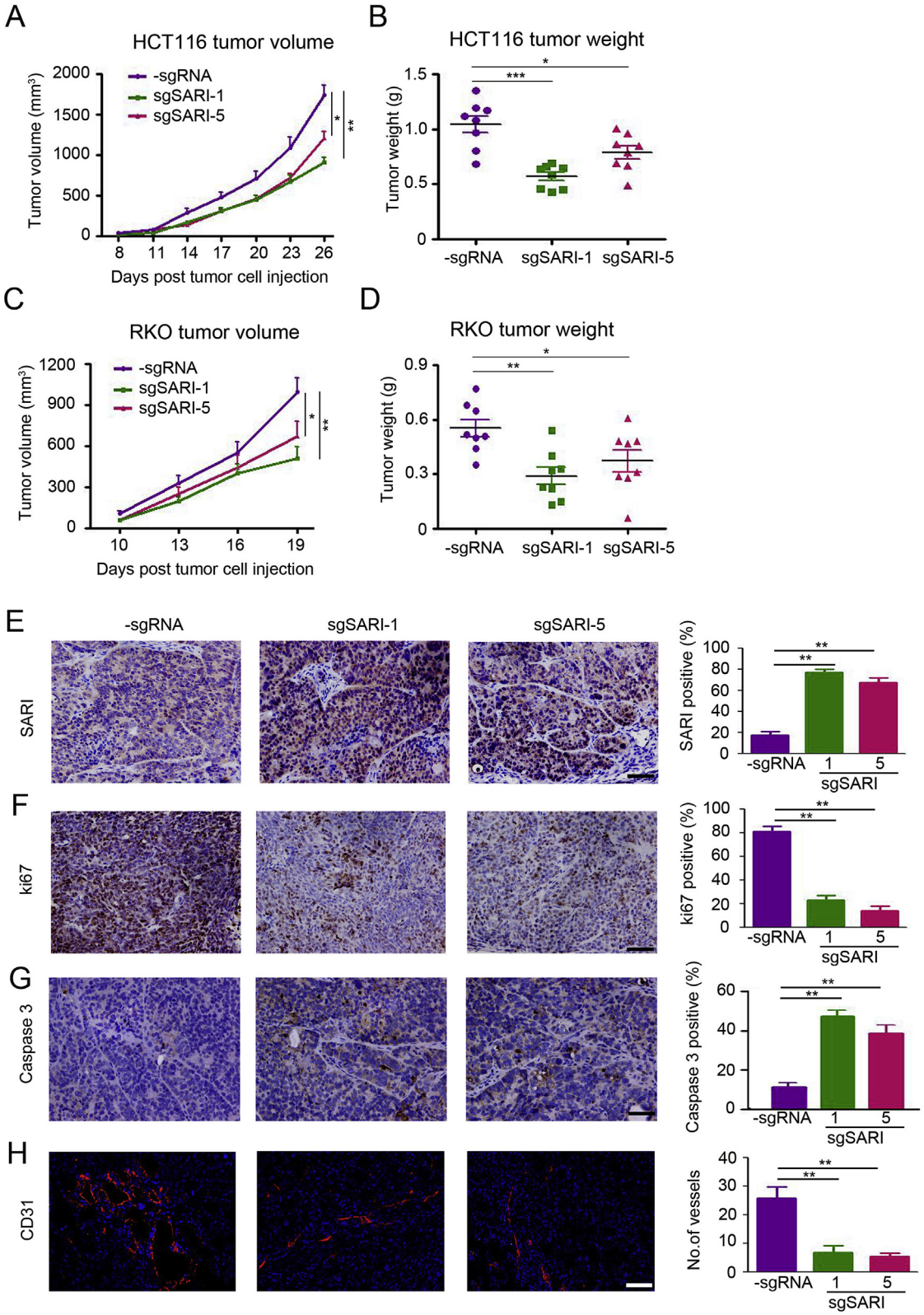

Fig. 5. Antitumour effect of the targeted demethylation of SARI *in vivo*. (A&B) Tumour volume and end-stage tumour weight after the injection of 5×10^6 HCT116 cells stably transfected with dCas9-multiGCN4/scFv-TET1CD-sgRNA, dCas9-multiGCN4/scFv-TET1CD-sgSARI-1, and dCas9-multiGCN4/scFv-TET1CD-sgSARI-5 (n = 5). (C&D) Tumour volume and end-stage tumour weight after the injection of 5×10^6 RKO cells stably transfected with dCas9-multiGCN4/scFv-TET1CD-sgRNA, dCas9-multiGCN4/scFv-TET1CD-sgSARI-1, and dCas9-multiGCN4/scFv-TET1CD-sgSARI-5 (n = 5). (E&F) Immunohistochemical staining of SARI and Ki67 in HCT116 tumours. The percentages of SARI- and Ki67-positive cells were analysed (n = 4, Scale bar = 100 μm). (G) Detection of apoptotic cells in HCT116 tumours by a caspase 3 staining. The numbers of caspase 3 positive cells per frame were counted and analysed (n = 4, Scale bar = 100 μm). (H) Staining for CD31 in HCT116 tumours (red). The cell nuclei were stained by DAPI (blue). The number of vessels per frame were counted and analysed (n = 4, Scale bar = 100 μm). (*p < 0.05; **p < 0.01; ***p < 0.001, compared with the sgRNA group).

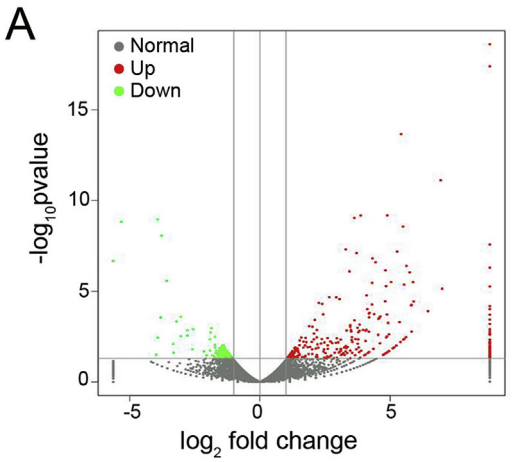

B

Deregulated KEGG pathways by SARI demethylation

Term	Gene
Apoptosis	TUBA3D; PRF1; HRAS; ATM; TUBA1A
Cell Cycle	SFN; CDK7; ATM; YWHAE
PI3K-Akt signaling pathway	COL6A3; THBS2; CREB5; GNG11; HRAS
	CREB3L1; COL4A2; SOS2; PGF; YWHAE; NGFR
MAPK signaling pathway	PRKACB; PTPN7; HRAS; MAPK8IP1; SOS2
	HSPA2; TAOK1; RRAS
VEGF signaling pathway	HRAS; SPHK1; VEGF
Ubiquitin mediated proteolysis	HERC2; TCEB2

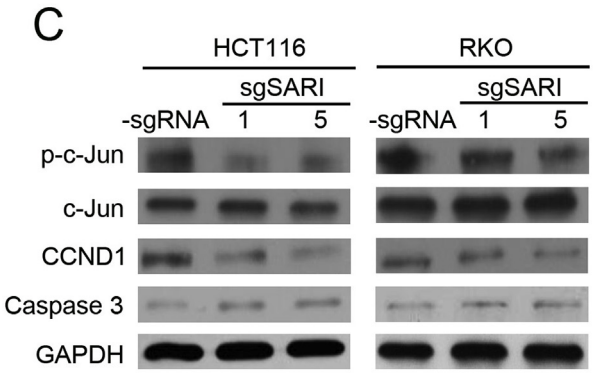

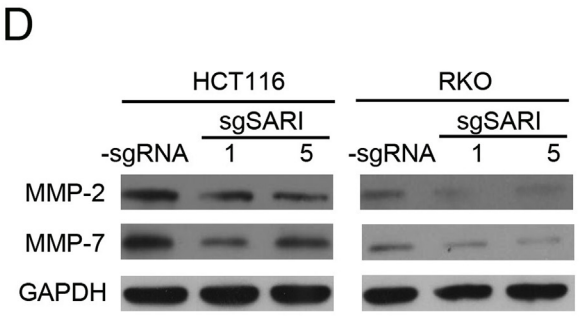

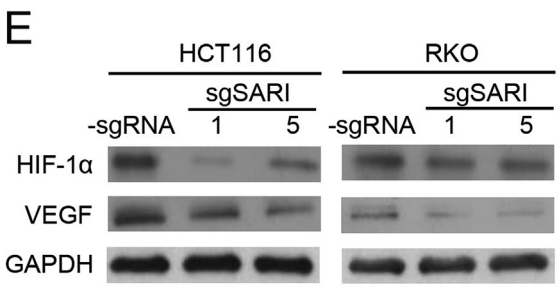

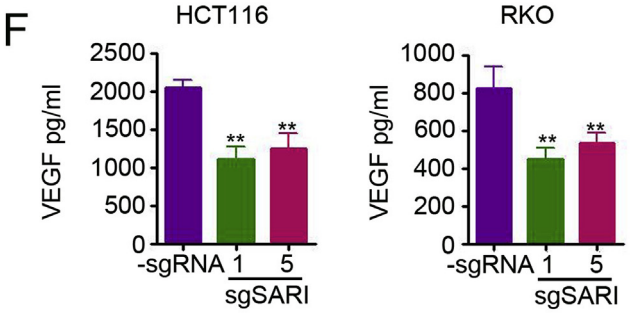

Fig. 6. Expression of downstream targets after the targeted demethylation of SARI. (A) Deregulated genes in HCT116 cells after the targeted demethylation of SARI. (B) Deregulated KEGG pathways in HCT116 cells after the targeted demethylation of SARI. (C) Western blotting analysis of p-*c*-Jun, c-Jun, CCND1, and Caspase 3 expression in HCT116 and RKO cells transfected with dCas9-multiGCN4/scFv-TET1CD-sgRNA, dCas9-multiGCN4/scFv-TET1CD-sgSARI-1, and dCas9-multiGCN4/scFv-TET1CD-sgSARI-5. (D) Western blotting analysis of MMP-2 and MMP-7 expression in HCT116 and RKO cells after transfection. (E) Western blotting analysis of HIF-1α and VEGF expression in HCT116 and RKO cells after transfection. (F) Supernatants from HCT116 and RKO cells after transfection were collected for VEGF detection by ELISA (n = 4, **p < 0.01, compared with the sgRNA group).

4. Discussion

Our results demonstrated that DNA methylation causes SARI inactivation in colon cancer and SARI methylation is a prognostic indicator in colon cancer. Furthermore, we constructed a dCas9-multiGCN4/scFv-TET1CD-sgRNA-based targeted demethylation system (dCas9-multiGCN4/scFv-TET1CD-sgSARI) and demonstrated that it precisely and specifically demethylates specific regions of SARI and results in the substantial activation of SARI expression. Further *in vitro* and *in vivo* analyses confirmed the anti-tumour role of dCas9-multiGCN4/scFv-TET1CD-sgSARI by regulating tumour proliferation, apoptosis, and angiogenesis.

DNA methylation of promoters and other gene regulatory regions frequently results in the inactivation of gene expression, and the methylation-mediated silencing of transcription has been linked to the downregulation of tumour suppressor genes [32,33]. Gene expression levels increase after the induction of demethylation in these regions. Thus, DNA methylation is a potential epigenetic biomarker of various types of cancer [34,35]. SARI expression is downregulated in most malignant tissues of various cancers [26,27,30]. We observed a high methylation rate of SARI CpG sites and an increase in SARI expression by the general demethylating agents DAC and AZA in colon cancer cells, which is consistent a previous study that indicated that SARI mRNA expression in childhood medulloblastoma cells was restored by a DNA methyltransferase inhibitor zebularine [36]. The highest level of demethylation was observed at CpG sites proximal to the sgSARI-1 and sgSARI-5 binding site, accompanied by a substantial increase in SARI expression. A strong correlation between SARI expression and SARI methylation was further detected in colon tissues from patients with colon cancer, which confirmed that the downregulation of SARI expression is mediated by SARI promoter methylation. Moreover, consistent with the inverse correlation between SARI expression and poor

prognosis in several cancers [30,37], we also demonstrated the predictive role of SARI methylation for survival in patients with colon cancer. Collectively, DNA methylation is the major cause of SARI inactivation in malignant tissues.

Owing to the undesirable effects caused by the global demethylation process, DAC and AZA faced the serious challenges in clinical applications [7,8]. Therefore, developing targeted demethylation strategy is necessary and urgent. ZFNs, TALEs, or the CRISPR-Cas9 system can be used as targeting domains during epigenome editing [38]. TALE-based systems benefit from their easy assembly and targeting in comparison with ZFNs [10,39]. However, the limited sensitivity to CpG methylation makes the TALE-based system inherently unsuitable for the modification of mammalian gene promoter methylation [40]. Owing to its efficiency, targeting specificity by gRNAs, and insensitivity to CpG methylation, the CRISPR-Cas9 system seems to be the best choice for epigenome editing [11,13,41]. In the present study, a dCas9-based system was developed using TET1CD as the functional domain in a single expression vector. Our results demonstrated that dCas9-multiGCN4/scFv-TET1CD-sgSARI-1 and -5 could efficiently activate endogenous SARI expression by the targeted demethylation of the *SARI* promoter. Moreover, a scoring system [31] for off-target predictions also confirmed the specificity of dCas9-multiGCN4/scFv-TET1CD-sgSARI-1 and -5 on demethylation of the *SARI* promoter. Therefore, dCas9-multiGCN4/scFv-TET1CD-sgSARI is an efficient and specific tool to activate endogenous SARI expression by targeted demethylation of the *SARI* promoter.

SARI acts as a tumour suppressor in various cancers [18,27,30,42]. Thus, based on the specificity and efficiency of dCas9-multiGCN4/scFv-TET1CD-sgSARI on SARI demethylation and the restoration of endogenous SARI expression, we next investigated the potential anti-tumour roles of dCas9-multiGCN4/scFv-TET1CD-sgSARI in colon cancer *in vitro* and *in vivo*. Our results suggested that dCas9-multiGCN4/scFv-TET1CD-sgSARI inhibits tumour growth via the induction of apoptosis and the inhibition of proliferative and angiogenic effects *in vitro* and *in vivo*, consistent with the results of previous studies [27,30]. C-Jun is a well-known direct and downstream target of SARI during the regulation of cell proliferation and apoptosis [18,42]. In our study, we also detected the inhibition of p-*c*-Jun expression, following CCND1 downregulation and Caspase 3 upregulation by dCas9-multiGCN4/scFv-TET1CD-sgSARI. Furthermore, MMP-2 and MMP-7 downregulation may be responsible for the inhibition of the invasion and migration ability in dCas9-multiGCN4/scFv-TET1CD-sgSARI-transfected colon cancer cells, as previously indicated [27]. dCas9-multiGCN4/scFv-TET1CD-sgSARI also inhibited tumour angiogenesis by inhibiting HIF-1α and VEGF expression, consistent with our previous results [30]. Therefore, the activation of endogenous SARI expression by the targeted demethylation of the *SARI* promoter had an anti-tumour role by regulating downstream target expression, similar to the effects of overexpressed exogenous SARI. However, for acquiring the more sufficient therapeutic effect on colon cancer, an efficient delivery system should be used to deliver dCas9-multiGCN4/scFv-TET1CD-sgSARI into cells. Viral-based delivery system, including lentivirus and adeno-associated viruses (AAVs) would be the best choice, according to the effectiveness [43]. The further study should be performed to determine the possibility.

Collectively, specific demethylation of the *SARI* promoter and the restoration of endogenous SARI expression by dCas9-multiGCN4/scFv-TET1CD-SARI should have therapeutic applications for colon cancer and perhaps for other cancers.

Author contributions

Qin Wang and Lei Dai performed most of the experiments with assistance from Yuan Wang, Jie Deng, Yi Lin. Qingnan Wang. Hongxin Deng and Lei Dai were involved in study concept design, analysis and interpretation of data, drafting of the manuscript and critical revision of the manuscript for important intellectual content. Lei Dai and Hongxin Deng were involved in obtained funding. Zida Ma, Chao Fang, Lie Yang and Zongguang Zhou were involved in clinical samples collected. Huiling Wang, Gang Shi, Lin Cheng, Yi Liu and Xiaolan Su were involved in animal study. Shuang Chen, Junshu Li and Zhexu Dong were involved in the molecular experiments. Shuang Zhang, Yang Yang, Ming Jiang and Meijuan Huang were involved in technical support and analysis and interpretation of data. Dechao Yu and Yuquan Wei were involved in obtained funding and study supervision.

Conflicts of interest

All authors declare that there are no conflicts of interest.

Appendix A. Supplementary data

Supplementary data to this article can be found online at https://doi.org/10.1016/j.canlet.2019.01.040.

Grant support

This study was supported by the National Natural Science Foundation of China Program grant (no. 81702349) and the National Key R&D Program of China grant (2017YFA0105702) and the National Science and Technology Major Project of China grant (2017ZX09304023) and the Postdoctoral Foundation of China (2017M612974) and the Fundamental Research Funds for the Central Universities (2017SCU12033).

References

[1] G.L. Brien, D.G. Valerio, S.A. Armstrong, Exploiting the epigenome to control cancer-promoting gene-expression programs, Cancer Cell 29 (2016) 464–476.
[2] W.A. Flavahan, E. Gaskell, B.E. Bernstein, Epigenetic Plasticity and the Hallmarks of Cancer, (2017), p. 357.
[3] A. Kinnaird, S. Zhao, K.E. Wellen, E.D. Michelakis, Metabolic control of epigenetics in cancer, Science (New York, N.Y.) 16 (2016) 694–707.
[4] J.S. You, P.A. Jones, Cancer genetics and epigenetics: two sides of the same coin? Cancer Cell 22 (2012) 9–20.
[5] G. Garcia-Manero, E. Jabbour, G. Borthakur, S. Faderl, Z. Estrov, H. Yang, S. Maddipoti, L.A. Godley, N. Gabrail, J.G. Berdeja, A. Nadeem, L. Kassalow, H. Kantarjian, Randomized open-label phase II study of decitabine in patients with low- or intermediate-risk myelodysplastic syndromes, J. Clin. Oncol.: Offic. J. Am. Soc. Clin. Oncol. 31 (2013) 2548–2553.
[6] H.M. Kantarjian, X.G. Thomas, A. Dmoszynska, A. Wierzbowska, G. Mazur, J. Mayer, J.P. Gau, W.C. Chou, R. Buckstein, J. Cermak, C.Y. Kuo, A. Oriol, F. Ravandi, S. Faderl, J. Delaunay, D. Lysak, M. Minden, C. Arthur, Multicenter, randomized, open-label, phase III trial of decitabine versus patient choice, with physician advice, of either supportive care or low-dose cytarabine for the treatment of older patients with newly diagnosed acute myeloid leukemia, J. Clin. Oncol.: Offic. J. Am. Soc. Clin. Oncol. 30 (2012) 2670–2677.
[7] M.A. Dawson, The cancer epigenome: concepts, challenges, and therapeutic opportunities, Science (New York, N.Y.) 355 (2017) 1147–1152.
[8] P.A. Northcott, S.M. Pfister, D.T. Jones, Next-generation (epi)genetic drivers of childhood brain tumours and the outlook for targeted therapies, Lancet Oncol. 16 (2015) e293–302.
[9] M.H. Porteus, D. Carroll, Gene targeting using zinc finger nucleases, Nat. Biotechnol. 23 (2005) 967–973.
[10] M.L. Maeder, J.F. Angstman, M.E. Richardson, S.J. Linder, V.M. Cascio, S.Q. Tsai, Q.H. Ho, J.D. Sander, D. Reyon, B.E. Bernstein, J.F. Costello, M.F. Wilkinson, J.K. Joung, Targeted DNA demethylation and activation of endogenous genes using programmable TALE-TET1 fusion proteins, Nat. Biotechnol. 31 (2013) 1137–1142.
[11] S.E. Jacobsen, X. Xu, Y. Tao, X. Gao, L. Zhang, X. Li, W. Zou, K. Ruan, F. Wang, G.L. Xu, R. Hu, A CRISPR-based approach for targeted DNA demethylation, Proc. Natl. Acad. Sci. U. S. A 2 (2016) 16009.
[12] S. Morita, H. Noguchi, T. Horii, K. Nakabayashi, M. Kimura, K. Okamura, Targeted DNA demethylation in vivo using dCas9-peptide repeat and scFv-TET1 catalytic domain fusions, Nat. Biotechnol. 34 (2016) 1060–1065.
[13] A. Vojta, P. Dobrinic, V. Tadic, L. Bockor, P. Korac, B. Julg, M. Klasic, V. Zoldos, Repurposing the CRISPR-Cas9 system for targeted DNA methylation, Nucleic Acids Res. 44 (2016) 5615–5628.
[14] H. Sasaki, Y. Matsui, Epigenetic events in mammalian germ-cell development: reprogramming and beyond, Nat. Rev. Genet. 9 (2008) 129–140.
[15] X. Yin, Y. Xu, Structure and function of TET enzymes, Adv. Exp. Med. Biol. 945 (2016) 275–302.
[16] X.S. Liu, H. Wu, M. Krzisch, X. Wu, J. Graef, J. Muffat, D. Hnisz, C.H. Li, B. Yuan,

C. Xu, Y. Li, D. Vershkov, A. Cacace, R.A. Young, R. Jaenisch, M. Okada, M. Kanamori, K. Someya, H. Nakatsukasa, A. Yoshimura, Rescue of fragile X syndrome neurons by DNA methylation editing of the FMR1 gene stabilization of Foxp3 expression by CRISPR-dcas9-based epigenome editing in mouse primary T cells, Cell 172 (2018) 979-992.e976.

[17] J. Gallego-Bartolome, J. Gardiner, W. Liu, A. Papikian, B. Ghoshal, H.Y. Kuo, J.M. Zhao, D.J. Segal, Targeted DNA demethylation of the Arabidopsis genome using the human TET1 catalytic domain, Nucleic Acids Res. 115 (2018) E2125-e2134.

[18] Z.Z. Su, S.G. Lee, L. Emdad, I.V. Lebdeva, P. Gupta, K. Valerie, D. Sarkar, P.B. Fisher, Cloning and characterization of SARI (suppressor of AP-1, regulated by IFN), Proc. Natl. Acad. Sci. U. S. A 105 (2008) 20906–20911.

[19] T.L. Murphy, R. Tussiwand, K.M. Murphy, Specificity through cooperation: BATF-IRF interactions control immune-regulatory networks, Nature reviews, Immunology 13 (2013) 499–509.

[20] S. Roy, R. Guler, S.P. Parihar, S. Schmeier, B. Kaczkowski, H. Nishimura, J.W. Shin, Y. Negishi, M. Ozturk, R. Hurdayal, A. Kubosaki, Y. Kimura, M.J. de Hoon, Y. Hayashizaki, F. Brombacher, H. Suzuki, Batf2/Irf1 induces inflammatory responses in classically activated macrophages, lipopolysaccharides, and mycobacterial infection, J. Immunol. (Baltimore, Md.: 1950) 194 (2015) 6035–6044.

[21] S. Kitada, H. Kayama, BATF2 inhibits immunopathological Th17 responses by suppressing Il23a expression during Trypanosoma cruzi infection, J. Exp. Med. 214 (2017) 1313–1331.

[22] Q. Chen, Y. Gu, S. Zhang, H. Deng, Effects and mechanisms of action of SARI on androgen-independent prostate cancer (DU145) cells, Tumour Biol. J. Int. Soc. Oncodevelopmental Biol. Med. 37 (12) (2016) 16141–16149.

[23] R. Dash, P. Bhoopathi, S.K. Das, S. Sarkar, L. Emdad, S. Dasgupta, D. Sarkar, P.B. Fisher, Novel mechanism of MDA-7/IL-24 cancer-specific apoptosis through SARI induction, Cancer Res. 74 (2014) 563–574.

[24] R. Guler, S. Roy, H. Suzuki, F. Brombacher, Targeting Batf2 for infectious diseases and cancer, Oncotarget 6 (2015) 26575–26582.

[25] Q. Huang, Y. Yang, X. Li, S. Huang, Transcription suppression of SARI (suppressor of AP-1, regulated by IFN) by BCR-ABL in human leukemia cells, Tumour Biol.: J. Int. Soc. Oncodevelopmental Biol. Med. 32 (2011) 1191–1197.

[26] Y. Huang, J. Zhou, Y. Huang, J. He, Y. Wang, C. Yang, D. Liu, L. Zhang, F. He, SARI, a novel target gene of glucocorticoid receptor, plays an important role in dexamethasone-mediated killing of B lymphoma cells, Cancer Lett. 373 (2016) 57–66.

[27] Z. Liu, P. Wei, Y. Yang, W. Cui, B. Cao, C. Tan, B. Yu, R. Bi, K. Xia, W. Chen, Y. Wang, Y. Zhang, X. Du, X. Zhou, BATF2 deficiency promotes progression in human colorectal cancer via activation of HGF/MET signaling: a potential rationale for combining MET inhibitors with IFNs, Clin. Cancer Res.: Offic. J. Am. Assoc. Canc. Res. 21 (2015) 1752–1763.

[28] C. Wang, Y. Su, L. Zhang, M. Wang, J. You, X. Zhao, Z. Zhang, J. Liu, X. Hao, The function of SARI in modulating epithelial-mesenchymal transition and lung adenocarcinoma metastasis, PLoS One 7 (2012) e38046.

[29] H. Kanemaru, F. Yamane, K. Fukushima, T. Matsuki, T. Kawasaki, I. Ebina, K. Kuniyoshi, H. Tanaka, K. Maruyama, K. Maeda, T. Satoh, S. Akira, Antitumor effect of Batf2 through IL-12 p40 up-regulation in tumor-associated macrophages, Proc. Natl. Acad. Sci. U. S. A 114 (2017) E7331–e7340.

[30] L. Dai, X. Cui, X. Zhang, L. Cheng, Y. Liu, Y. Yang, P. Fan, Q. Wang, Y. Lin, J. Zhang, C. Li, Y. Mao, Q. Wang, X. Su, S. Zhang, Y. Peng, H. Yang, X. Hu, J. Yang, M. Huang, R. Xiang, D. Yu, Z. Zhou, Y. Wei, H. Deng, SARI inhibits angiogenesis and tumour growth of human colon cancer through directly targeting ceruloplasmin, Nat. Commun. 7 (2016) 11996.

[31] T. Mlambo, S. Nitsch, M. Hildenbeutel, M. Romito, M. Muller, C. Bossen, S. Diederichs, T.I. Cornu, T. Cathomen, C. Mussolino, Designer epigenome modifiers enable robust and sustained gene silencing in clinically relevant human cells, Nucleic Acids Res. 46 (2018) 4456–4468.

[32] R. Dante, Y. Luo, C.J. Wong, A.M. Kaz, S. Dzieciatkowski, K.T. Carter, S.M. Morris, J. Wang, J.E. Willis, K.W. Makar, C.M. Ulrich, J.D. Lutterbaugh, M.J. Shrubsole, W. Zheng, S.D. Markowitz, W.M. Grady, Differences in DNA methylation signatures reveal multiple pathways of progression from adenoma to colorectal cancer, EMBO Mol. Med. 147 (2014) 418–429 e418.

[33] A. Koch, S.C. Joosten, Z. Feng, T.C. de Ruijter, M.X. Draht, V. Melotte, K.M. Smits, J. Veeck, J.G. Herman, L.V. Neste, W.V. Criekinge, T. De Meyer, M.V. Engeland, J.H. Kim, S.M. Dhanasekaran, J.R. Prensner, X. Cao, D. Robinson, S. Kalyana-Sundaram, C. Huang, S. Shankar, X. Jing, M. Iyer, M. Hu, L. Sam, C. Grasso, C.A. Maher, N. Palanisamy, R. Mehra, H.D. Kominsky, J. Siddiqui, J. Yu, Z.S. Qin, A.M. Chinnaiyan, Analysis of DNA methylation in cancer: location revisited Deep sequencing reveals distinct patterns of DNA methylation in prostate cancer, Nat. Rev. Clin. Oncol. 21 (2018) 1028–1041.

[34] T. Hinoue, D.J. Weisenberger, C.P. Lange, H. Shen, H.M. Byun, D. Van Den Berg, S. Malik, F. Pan, H. Noushmehr, C.M. van Dijk, R.A. Tollenaar, P.W. Laird, Genome-scale analysis of aberrant DNA methylation in colorectal cancer, Genome Res. 22 (2012) 271–282.

[35] J. Jeschke, M. Bizet, C. Desmedt, E. Calonne, S. Dedeurwaerder, S. Garaud, A. Koch, D. Larsimont, R. Salgado, G. Van den Eynden, K. Willard Gallo, G. Bontempi, M. Defrance, C. Sotiriou, F. Fuks, DNA methylation-based immune response signature improves patient diagnosis in multiple cancers, J. Clin. Invest. 127 (2017) 3090–3102.

[36] A.F. Andrade, K.S. Borges, V.K. Suazo, L. Geron, C.A. Correa, A.M. Castro-Gamero, E.J. de Vasconcelos, R.S. de Oliveira, L. Neder, J.A. Yunes, S. Dos Santos Aguiar, C.A. Scrideli, L.G. Tone, The DNA methyltransferase inhibitor zebularine exerts antitumor effects and reveals BATF2 as a poor prognostic marker for childhood medulloblastoma, Invest. N. Drugs 35 (2017) 26–36.

[37] R.J. Zhou, Z. Shi, K. Zhou, H.D. Wang, G.Q. Zhang, X.T. Li, J.P. Xu, Decreased SARI expression predicts poor prognosis of Chinese patients with non-small cell lung cancer, Int. J. Clin. Exp. Pathol. 6 (2013) 2056–2063.

[38] A. Straubeta, T. Lahaye, Zinc fingers, TAL effectors, or Cas9-based DNA binding proteins: what's best for targeting desired genome loci? Mol. Plant 6 (2013) 1384–1387.

[39] D.L. Bernstein, J.E. Le Lay, E.G. Ruano, K.H. Kaestner, TALE-mediated epigenetic suppression of CDKN2A increases replication in human fibroblasts, J. Clin. Invest. 125 (2015) 1998–2006.

[40] J. Valton, A. Dupuy, F. Daboussi, S. Thomas, A. Marechal, R. Macmaster, K. Melliand, A. Juillerat, P. Duchateau, Overcoming transcription activator-like effector (TALE) DNA binding domain sensitivity to cytosine methylation, J. Biol. Chem. 287 (2012) 38427–38432.

[41] T. Anton, S. Bultmann, Site-specific recruitment of epigenetic factors with a modular CRISPR/Cas system, Nucleus (Austin, Tex.) 8 (2017) 279–286.

[42] R. Dash, Z.Z. Su, S.G. Lee, B. Azab, H. Boukerche, D. Sarkar, P.B. Fisher, Inhibition of AP-1 by SARI negatively regulates transformation progression mediated by CCN1, Oncogene 29 (2010) 4412–4423.

[43] D. Ibraheem, A. Elaissari, H. Fessi, Gene therapy and DNA delivery systems, Int. J. Pharm. 459 (2014) 70–83.